Research Square

Preprints are preliminary reports that have not undergone peer review.
They should not be considered conclusive, used to inform clinical practice,
or referenced by the media as validated information.

Synthesis, Characterization, and Biological Evaluation of an N_4-Donor Schiff Base Zinc(II) Complex: Antibacterial, Antioxidant, Anticancer, and Molecular Docking Studies

M Periyannan

periyanna6@periyaruniversity.ac.in

Periyar University

G Anbarasu

Bharathiar University

D Gopi

Periyar University

R Rajavel

Periyar University

Research Article

Keywords: Schiff-base ligand, Zn (II)-Complex, Biological Studies, Molecular docking

Posted Date: November 20th, 2026

DOI: https://doi.org/10.21203/rs.3.rs-11659341/v1

License: This work is licensed under a Creative Commons Attribution 4.0 International License.
Read Full License

Additional Declarations: No competing interests reported.

Synthesis, Characterization, and Biological Evaluation of an N_4-Donor Schiff Base Zinc(II) Complex: Antibacterial, Antioxidant, Anticancer, and Molecular Docking Studies

M.Periyannan [1], G.Anbarasu [2], D.Gopi [3] , R. Rajavel*[1]

[1] Department of Chemistry, Bio-Inorganic Lab, Periyar University, Salem, 636 011, Tamil Nadu, India.
[2] B.Sc.,(Blended) Programme, Centre for International Affairs, Bharathiar University, Coimbatore-641 046, Tamil Nadu, India.
[3] Department of Chemistry, Periyar University, Salem, 636 011, Tamil Nadu, India.

Corresponding author E-mail: drrajavel@periyaruniversity.ac.in

Abstract

A new Schiff-base Zn (II) complex was created through the reaction of 2-aminopyridine with 4-chlorobenzaldehyde. The characterized Schiff-base ligand and Zn complex were analysed using several techniques, including UV-Vis, FTIR, 1H-NMR, 13C-NMR, Mass spectrometry, Powder XRD, TGA, XPS, CV and SEM-EDX. The Zn (II) complex's biological activities were assessed for antibacterial, antifungal, antioxidant, and anticancer effects. Antibacterial effects were examined against chosen Gram-positive and Gram-negative bacterial strains, and antifungal effects were assessed against Candida albicans. The DPPH radical-scavenging assay was utilized to assess antioxidant potential, while the anticancer activity was evaluated against MCF-7 breast cancer cells through the MTT assay. The findings suggest that the created Zn (II) Schiff-base complex demonstrates notable biological characteristics and could be a viable candidate for additional bioinorganic and medicinal chemistry research.

Keywords: Schiff-base ligand, Zn (II)-Complex, Biological Studies, Molecular docking

1.Introduction

Coordination chemistry deals with the formation, structure, bonding, and properties of metal–ligand complexes and provides an important foundation for the development of functional molecular systems with applications in catalysis, materials science, bioinorganic chemistry, and medicinal chemistry. Among the diverse ligand systems, Schiff bases containing the characteristic azomethine (–CH=N–) functionality have attracted considerable attention because of their facile synthesis, structural flexibility, and versatile coordination behavior. The presence of additional donor atoms such as nitrogen, oxygen, or sulfur allows Schiff bases to act as mono-, bi-, or multidentate ligands and to generate metal complexes with diverse

geometries and physicochemical properties. Their conjugated aromatic frameworks and tunable electronic characteristics have further contributed to their extensive investigation as biologically active compounds **[1–3]**. Zinc(II) is an essential trace element involved in numerous biological processes and possesses flexible coordination chemistry, enabling the formation of stable complexes with nitrogen-, oxygen-, and sulfur-donor ligands. Consequently, Zn(II) complexes have received increasing attention in bioinorganic and medicinal chemistry. The biological properties of zinc Schiff-base complexes are influenced by several factors, including the nature of the ligand, donor atoms, coordination geometry, electronic structure, and overall molecular architecture **[4–6]**. In particular, N-donor Schiff-base systems are attractive because they can provide a defined coordination environment around the Zn(II) center and facilitate systematic investigation of structure–property relationships. Protein binding is an important aspect of understanding the biological behavior of coordination compounds. Bovine serum albumin (BSA), a major plasma protein, is frequently employed as a model protein for investigating the interaction of bioactive molecules with serum albumins. Binding studies can provide information concerning affinity, interaction mode, and possible transport behavior of metal complexes in biological systems. Recent investigations of Zn(II) Schiff-base complexes have demonstrated their interactions with BSA using spectroscopic and molecular-modelling approaches **[7,8]**. The biological assessment of Schiff-base metal complexes commonly involves antimicrobial, antioxidant, and anticancer investigations. Antibacterial evaluation against representative Gram-positive and Gram-negative organisms provides information about the potential of the compounds to inhibit bacterial growth, while antifungal studies against pathogenic fungi such as *Candida albicans* provide an additional measure of their antimicrobial spectrum **[9,10]**. Antioxidant properties can also be evaluated using the 2,2-diphenyl-1-picrylhydrazyl (DPPH) radical-scavenging assay, which is widely used to assess the free-radical-scavenging ability of Schiff bases and their metal complexes **[11]**. Cancer remains a major health challenge and continues to stimulate the development of new molecular systems with potential antiproliferative properties. Metal coordination provides an approach for modifying the biological characteristics of organic ligands and has therefore been investigated in the development of potential anticancer compounds. Schiff-base metal complexes have been evaluated against several human cancer cell lines, including MCF-7 breast cancer cells. The MTT cell-viability assay is commonly employed to investigate the cytotoxic effects of such compounds **[12]**. As a continuation of this paper of Schiff-base ligand (E)-1-(4-chlorophenyl)-N-(pyridin-2-yl) methenamine and Zn(II) complex and their structural features were addressed. The biological potential of the Zn(II)

complex was investigated through antibacterial studies against selected Gram-positive and Gram-negative bacterial strains, antioxidant activity using the DPPH radical-scavenging assay, and anticancer activity against MCF-7 breast cancer cells using the MTT assay and explore molecular docking interactions with target proteins

2.EXPERIMENTAL SECTION

2.1.Materials and Methods

The chemical reagents 2-aminopyridine and 4-chlorobenzaldehyde were purchased from MS Scientific Chemicals & Instruments and used without further purification. 2,2-Diphenyl-1-picrylhydrazyl (DPPH) and 3-(4,5-dimethylthiazol-2-yl)-2,5-diphenyltetrazolium bromide (MTT) were obtained from Himedia Laboratories, India. The MCF-7 human breast cancer cell line was procured from the National Centre for Cell Science (NCCS), Pune, India. All solvents were dried and purified according to standard procedures. The progress of the reactions was monitored by thin-layer chromatography (TLC) using Merck precoated silica gel 60 F254 plates, and the spots were visualized under ultraviolet (UV) light or by exposure to iodine vapour. Melting points were determined using an Electrothermal 9200 melting point apparatus by the capillary tube method and are reported without correction. Fourier-transform infrared (FT-IR) spectra were recorded using a PerkinElmer FT-IR spectrometer equipped with a Bruker attenuated total reflectance (ATR) accessory over the wavenumber range of 400–4000 cm^{-1}. Nuclear magnetic resonance (NMR) spectra were recorded using a Bruker DRX spectrometer operating at 400 MHz, with dimethyl sulfoxide-d_6 (DMSO-d_6) as the solvent and tetramethyl silane (TMS) as the internal reference. High-resolution mass spectra (HRMS) were acquired using a Bruker Maxis 10138 Mass spectrometer. The elemental composition and chemical states of the synthesized Zn (II) complex were investigated using a Thermo Scientific K-Alpha X-ray photoelectron spectrometer (XPS; Model: K-Alpha-KAN9954133). The surface morphology and microstructural characteristics of the Zn (II) complex were examined using a scanning electron microscope (SEM; Zeiss, Germany). Powder X-ray diffraction (PXRD) patterns were recorded using a Bruker D8 Advance diffractometer equipped with Cu Kα radiation. Thermogravimetric analysis (TGA) was performed using a Q500 high-resolution thermogravimetric analyser (TA Instruments) at a heating rate of 2 °C min^{-1}.Electrochemical measurements were carried out using a CHI 760C electrochemical workstation with a conventional three-electrode cell configuration comprising a glassy carbon electrode (GCE) as the working electrode, an Ag/AgCl electrode as the reference electrode and a platinum wire as

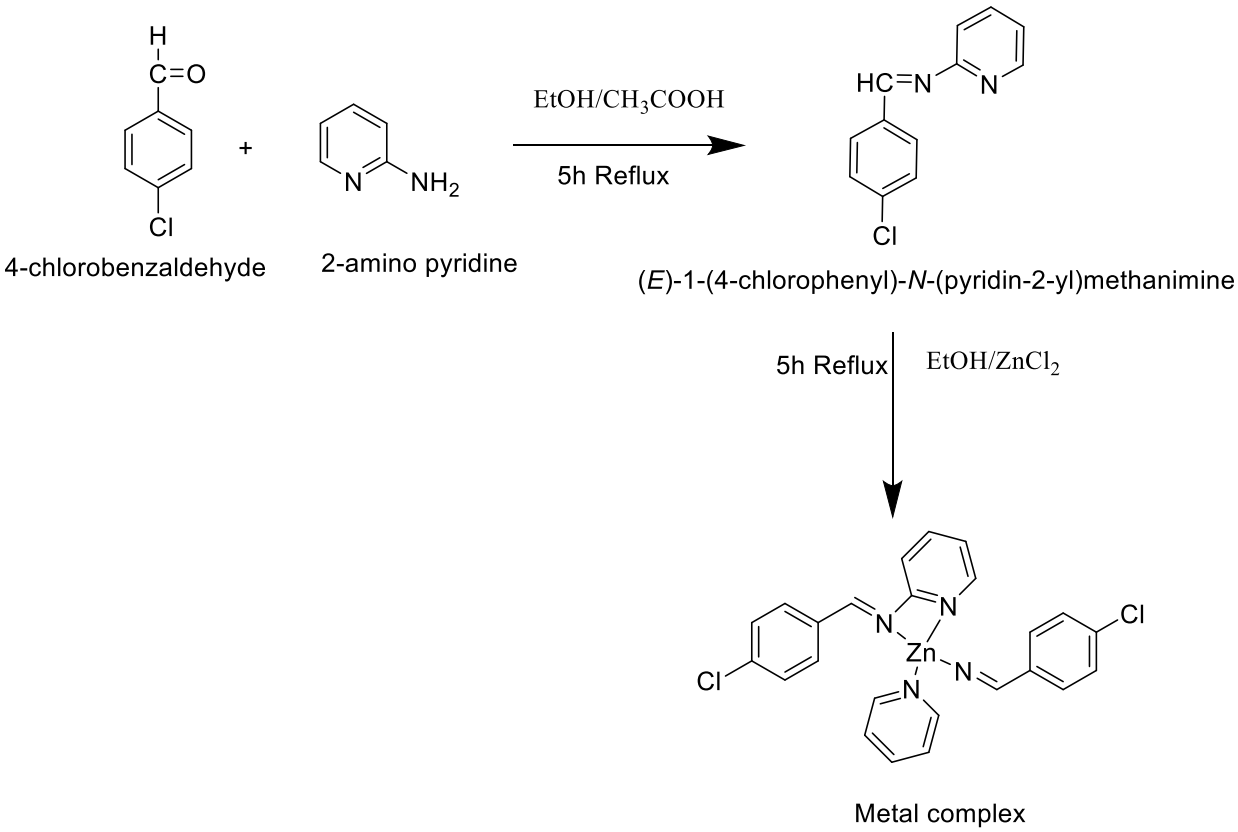
the counter electrode. The electrochemical behaviour of the synthesized compounds was investigated using cyclic voltammetry (CV).

2.2.Synthesis of Schiff Base Ligand and Zn Complex

A methanolic solution of 2-aminopyridine (0.471 g, 5 mmol) was mixed with a methanolic solution of 4-chlorobenzaldehyde (0.703 g, 5 mmol) in a 1:1 molar ratio in a round-bottom flask. An additional 10 mL of methanol was added dropwise, and the reaction mixture was stirred for 10 min to obtain a homogeneous solution. The resulting reaction mixture was heated under reflux for 5 h with continuous stirring and then allowed to cool to room temperature. The yellow precipitated Schiff-base ligand was collected by filtration, thoroughly washed with methanol and diethyl ether, and dried. Further purification was carried out by silica-gel column chromatography using a methanol–hexane solvent mixture as the eluent.

2.3.Synthesis of Zn complex

A hot methanolic solution of the Schiff-base ligand (0.433 g, 2 mmol) was prepared, and a methanolic solution of zinc chloride ($ZnCl_2$) (0.136 g, 1 mmol) was added slowly with continuous stirring to maintain a ligand-to-metal molar ratio of 2:1. The reaction mixture was refluxed with continuous stirring for 2 h Upon completion of the reaction, the mixture was allowed to cool to room temperature, yielding a pale-yellow precipitate. The precipitate was collected by filtration, washed thoroughly with methanol and diethyl ether, and dried under vacuum over anhydrous calcium chloride ($CaCl_2$).



Scheme 1. Preparation of Zn Complex

Table 1. Analytical and Physical data of Schiff base ligand and its Zn(II) Complex

Compounds	**Molecular Formula**	**Molecular Weight**	**Color**	**MP (^{0}C)**	**% Found (calculated)**				
					C	**H**	**N**	**Cl**	**Zn**
Ligand	$C_{12}H_9ClN_2$	216.05	Yellow	80	66.52	4.19	12.93	16.36	-
Zn-Complex	$C_{24}H_{19}Cl_2N_4Zn$	497.03	Pale-Yellow	230	57.68	3.83	11.21	14.19	13.08

The synthesized Zn(II) complex was found to be insoluble in water and most common organic solvents but exhibited good solubility in dimethylformamide (DMF) and dimethyl sulfoxide (DMSO).

2.4.Molar Conductance

The molar conductivity of the Zn(II) complex was measured at room temperature using a 10^{-3}M solution in DMF. The molar conductivity was found to be 20.11 S cm² mol⁻¹. This relatively low conductivity value suggests that the complex behaves as a non-electrolyte under the experimental conditions.

3.Results and Discussion

The formation of the investigated Schiff base ligand and its Zn- complex is represented in **Scheme 1.**

Characterization of the Schiff Base ligand and Zn- complex

3.1.UV-Vis Spectrum

The UV–Vi's absorption spectra of the Schiff base ligand and its Zn(II) complex were recorded in DMF at room temperature in the wavelength range of 200–800 nm. The Schiff base ligand showed absorption bands at 312 and 363 nm, which can be assigned to π→π* and n→π* transitions associated with the azomethine group. The Zn(II) complex showed absorption bands at 329 and 388 nm**[13-14].** The observed shifts in the absorption bands indicate coordination of the Schiff base ligand to the Zn(II) ion. Since Zn(II) has a d^{10} electronic configuration, d–d transitions are not expected. The observed bands are therefore mainly attributed to ligand-centered transitions, with possible charge-transfer contributions.

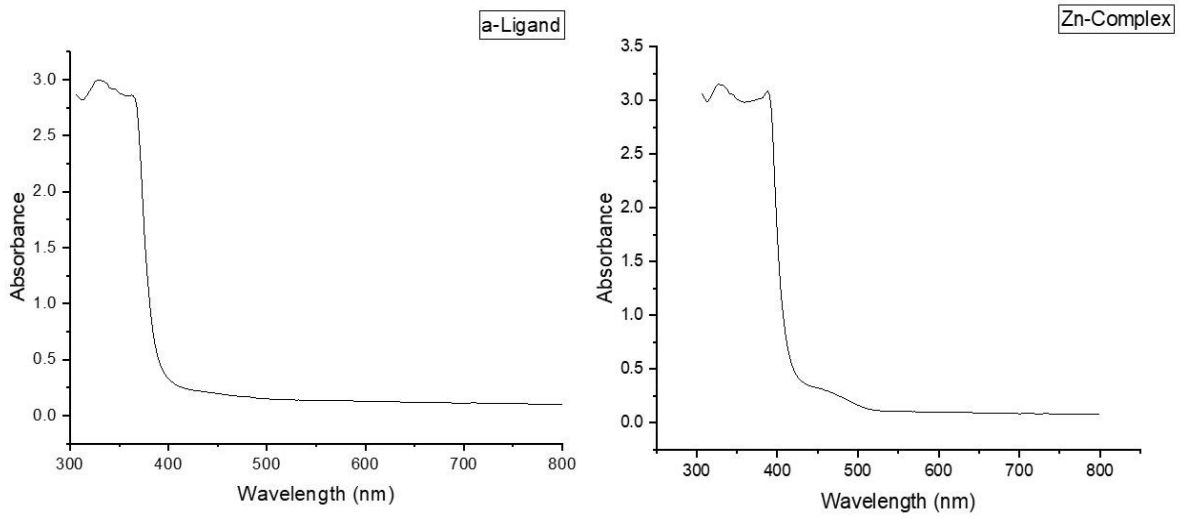


Figure. 1. UV–Vi's spectra of Ligand & Zn Complex.

3.2.FTIR Spectrum

Infrared spectrum (**Figure.2a,2b**) was registered between 400 and 4000 cm^{-1} revealing a band of medium absorption at 1637 cm-1, which can be attributed to the *ν*(C=N) azomethine stretching vibrations, confirming Schiff base connection. The compounds spectrum lacks of NH_2 stretching vibrations, which are associated with aldehyde and amine, respectively, indicating the formation of imine linkage needed for the development of Schiff base. The presence of aromatic *ν*(C-H) generated the stretching vibrations around 2890 cm^{-1}. This band shifted to 1600 cm−1 in the synthesized complex, indicating participation of the azomethine nitrogen in complexation. further supported by the formation of new bands in the regions

516cm^{-1} and which are due to m(Zn–N) bands, respectively **[15].** Therefore, the above arguments together with the elemental analyses indicated the Zn complex possibly have a Square Planner geometry.

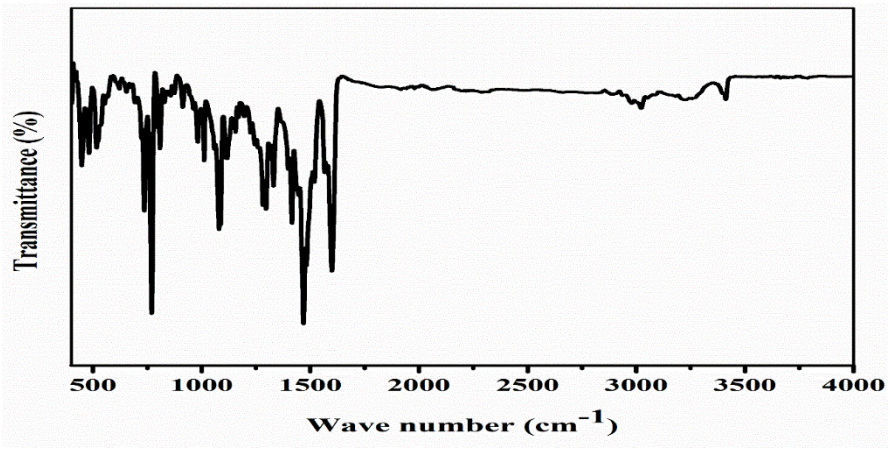


Figure 2.a. FTIR spectrum of the Schiff base Ligand

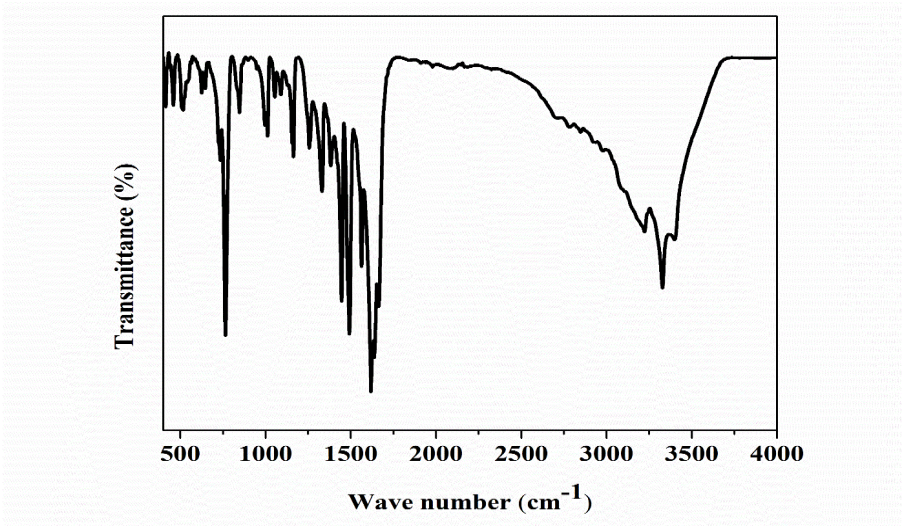


Figure. 2.b. FTIR spectrum of the Zn Complex

3.3. ^{1}H-NMR Spectrum

The ^{1}H-NMR spectrum of the derived compound (**Figure 3a**,) was obtained in DMSO-*d*6; signals seen between 8.07 and 9.20 ppm suggested alpha hydrogen for imine linkage (HC=N). The molecule has an aromatic ring, and the numerous signals seen in the range of 6.97-8.52 ppm are attributed to aromatic proton resonance. The ^{1}H NMR spectrum of the Zn(II) complex exhibits characteristic signals in the aromatic region, corresponding to the pyridine and 4-chlorophenyl moieties. The pyridine-ring protons appear in the chemical shift range of 6.90–8.59 ppm, whereas the aromatic protons of the 4-chlorophenyl rings are observed between 7.36 and 7.84 ppm. Notably, the azomethine proton (–CH=N–) signal undergoes an up field shift to 7.90 ppm upon complexation with Zn(II), compared with the corresponding signal of the free

Schiff-base ligand. This up field shift indicates the involvement of the azomethine nitrogen atom in coordination with the Zn(II) center **[16],** supporting the formation of the metal complex **(Figure 3c).**

3.4. ^{13}C NMR spectrum

The ^{13}C NMR spectrum of the synthesized Schiff-base ligand, recorded in DMSO-*d*6 **(Figure 3b),** exhibits characteristic resonances corresponding to the aromatic and imine carbon atoms. The signal at 155.01 ppm is attributed to the pyridine carbon adjacent to the nitrogen atom, while the resonance at 149.32 ppm is assigned to the azomethine carbon (C=N). The signal at 158.05 ppm is tentatively attributed to the carbon associated with the chlorine-substituted aromatic environment. The remaining signals, observed in the range of 112.27–134.10 ppm, are assigned to the aromatic carbon atoms of the pyridine and benzene rings. The predicted ^{13}C NMR spectrum of the Zn(II) complex **(Figure 3d)** exhibits characteristic resonances corresponding to the imine and aromatic carbon atoms of the pyridine and 4-chlorophenyl moieties. The signal at 174.5 ppm is tentatively assigned to the azomethine carbon (C=N), whereas the resonance at 149.8 ppm is attributed to a pyridine-ring carbon. The remaining aromatic carbon resonances are distributed over the range of 112.4–146.2 ppm, indicating the presence of the aromatic framework. Furthermore, the signal at 136.6 ppm may be attributed to the carbon bonded to chlorine in the 4-chlorophenyl moiety. These predicted chemical shifts are consistent with the expected carbon environments of the Schiff-base Zn(II) complex.

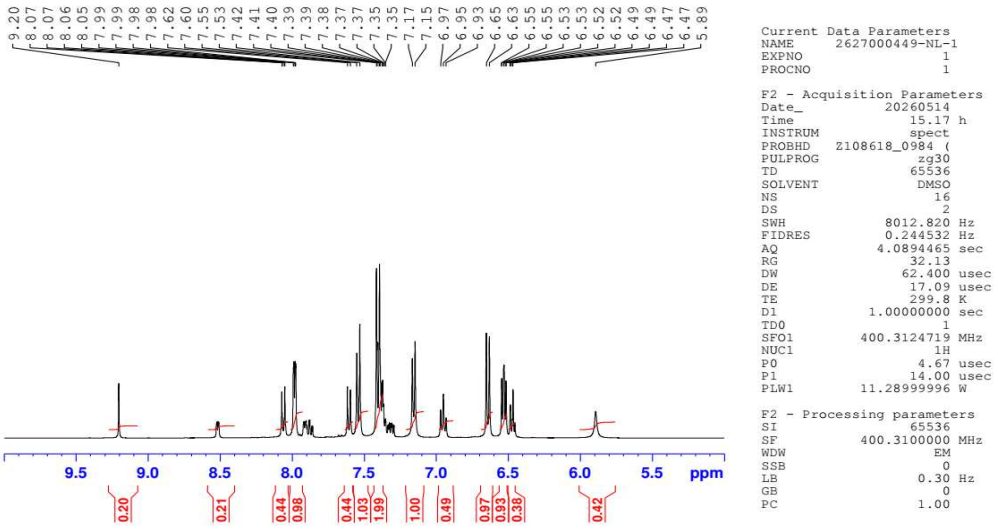


Figure 3a. ^{1}H-NMRspectrum of Schiff Base Ligand

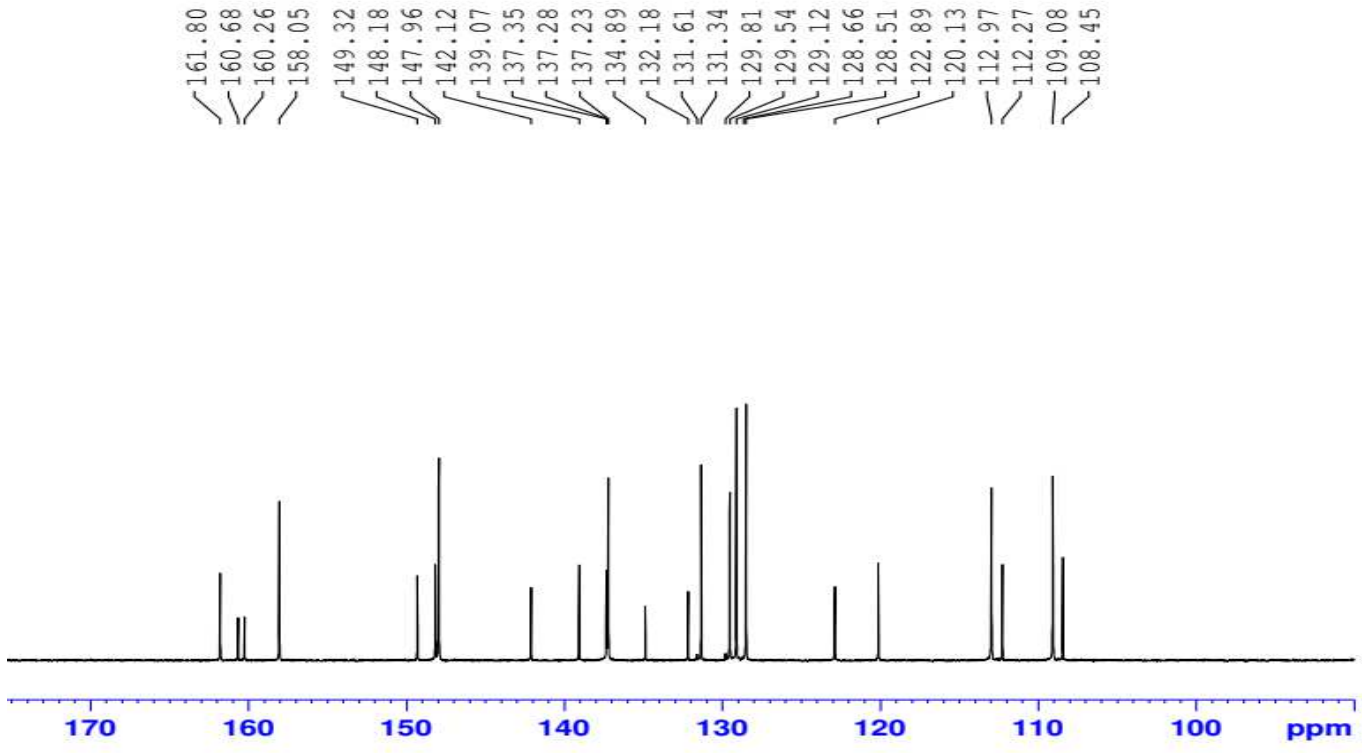


Figure.3b. ^{13}C-NMR -Schiff Base Ligand

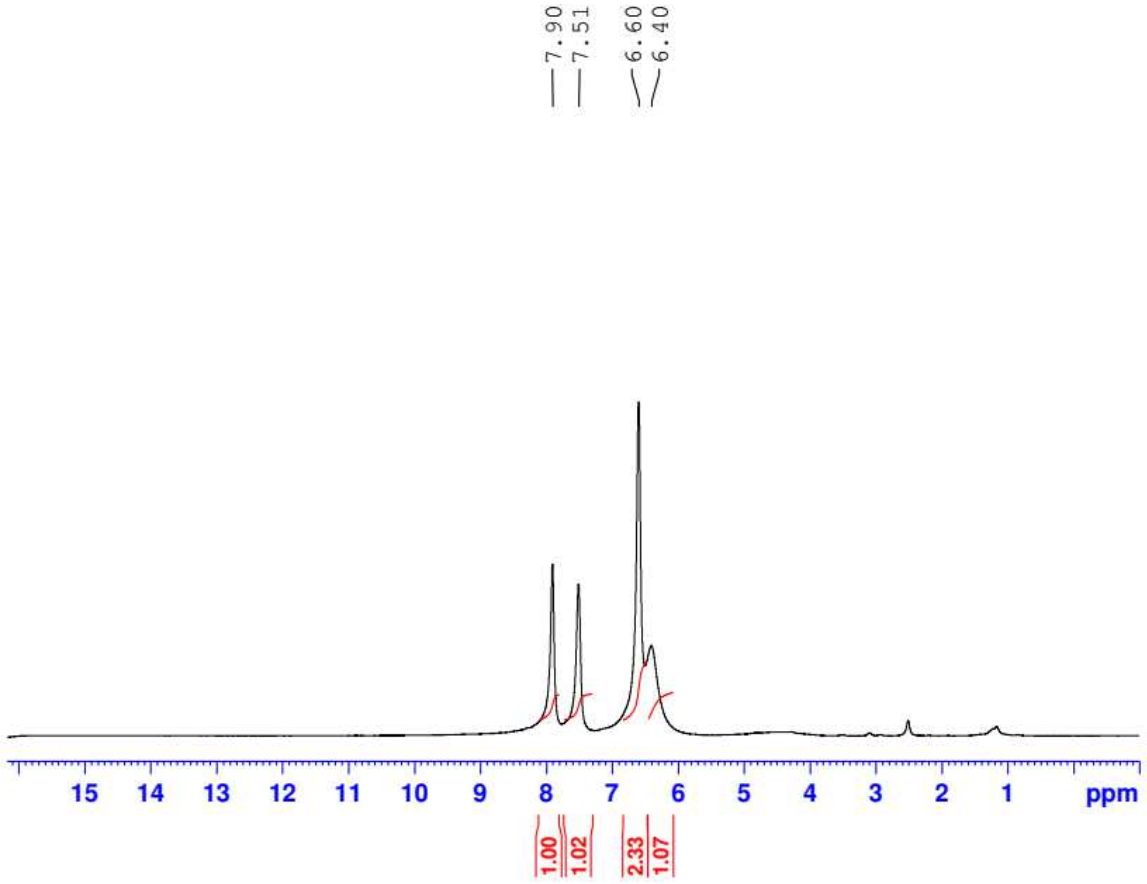


Figure.3c. ^{1}H-NMR -Zn-Complex

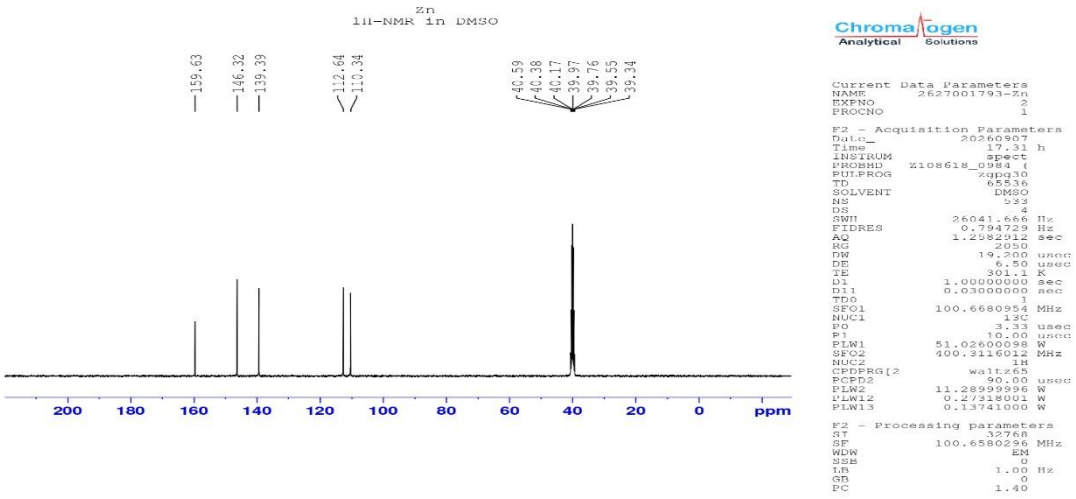


Figure.3d. ^{13}C-NMR - Zn-Complex

3.5.Mass Spectrum

Mass spectrometric analysis was performed to identify the molecular ion and the characteristic isotope peaks (M^+, M+1, M+2, etc.) of the synthesized compounds. The mass spectrum of the synthesized ligand was recorded and analyzed for structural confirmation, as shown in **(Figure 4a,4b).** The spectrum exhibited a molecular ion peak at m/z = 217, which is consistent with the expected molecular mass of the compound (216.67), with the observed difference attributable to the ionization and isotopic characteristics of the molecular species. This observation provides additional support for the proposed molecular structure. Similarly, the mass spectrum of the synthesized Zn(II) complex exhibited a prominent molecular ion peak at m/z = 497.

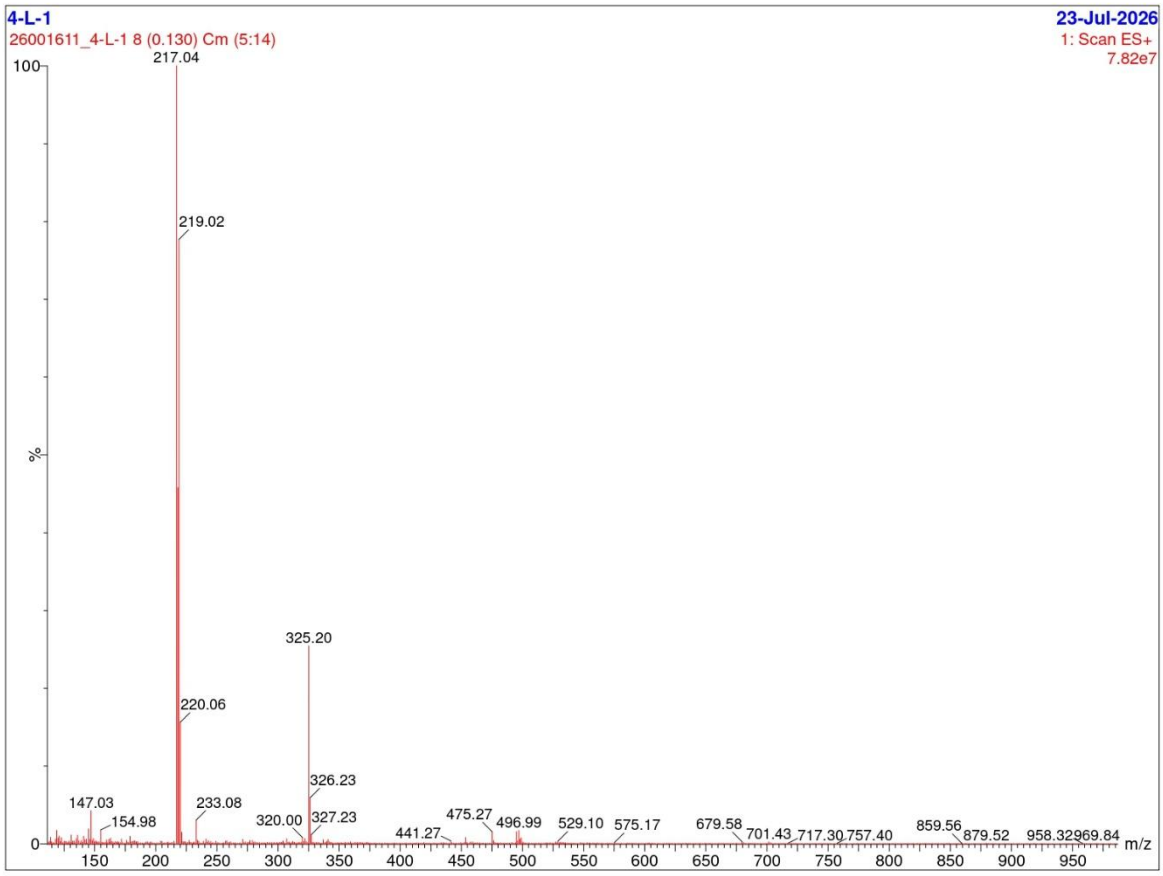


Figure 4a. Mass spectra of ligand

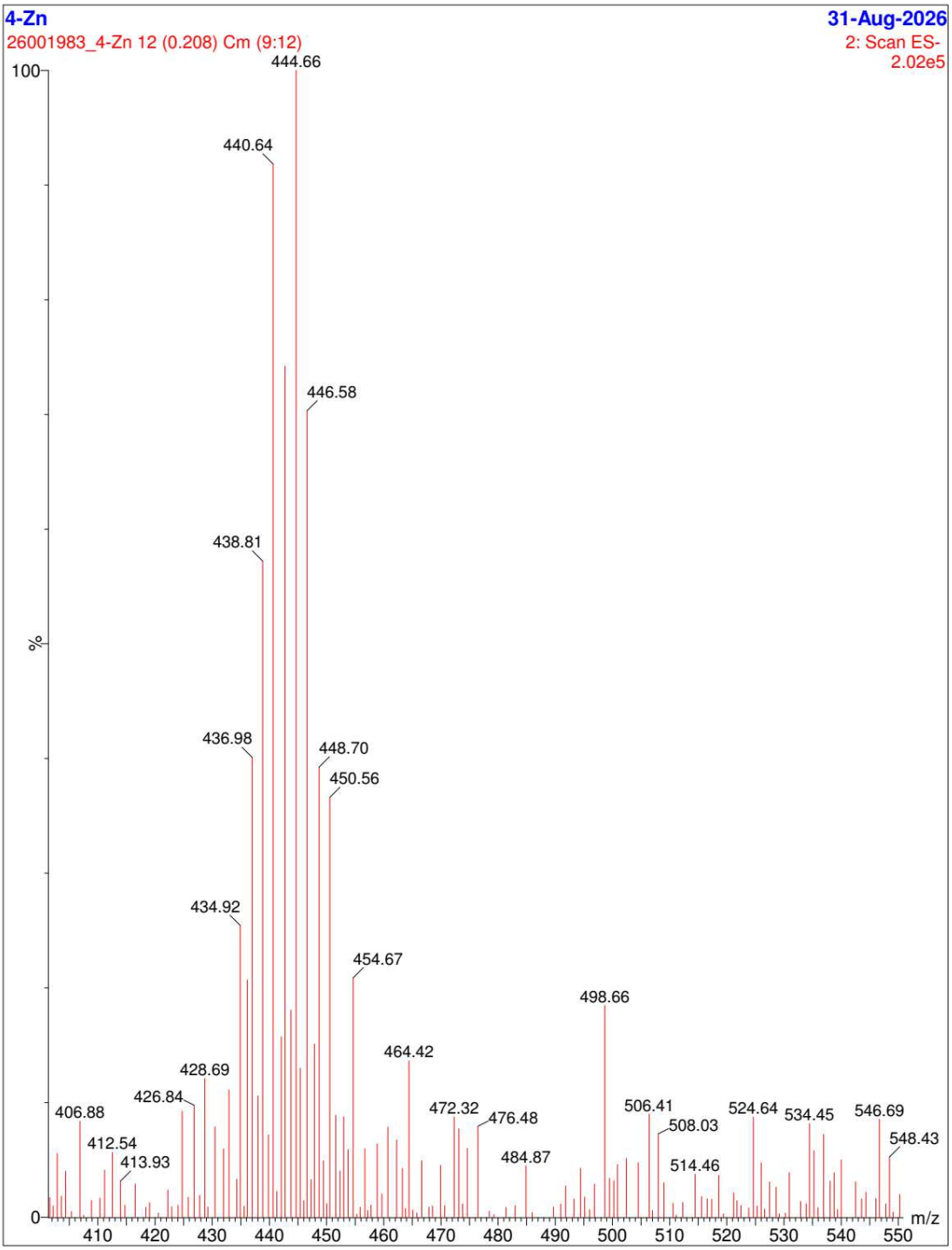


Figure 4b. Mass spectra of Zn Complex

3.6.Powder XRD

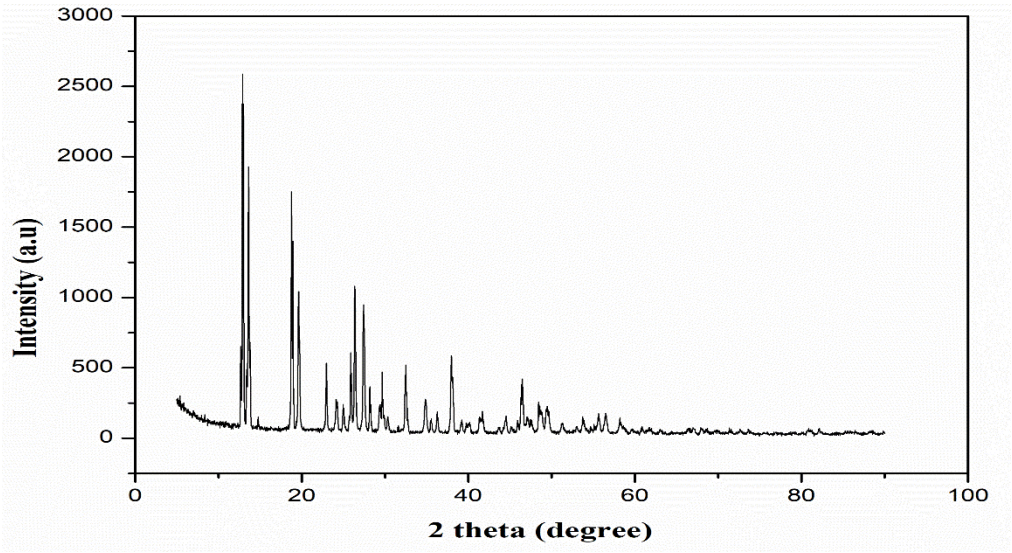


Figure.5 Powder X-ray diffraction of Zn(II) Metal Complex

The powder X-ray diffraction (PXRD) pattern of the synthesized Zn(II) Schiff-base complex exhibits several distinct diffraction peaks, indicating its crystalline nature. PXRD analysis is a valuable technique for investigating the crystalline structure, phase composition, and structural characteristics of newly synthesized metal complexes. The observed diffraction reflections provide useful information regarding the crystalline phases and can be employed to estimate the crystallite size and lattice parameters through appropriate analytical methods. Similar PXRD characteristics have been reported for Schiff-base-based Zn(II) complexes. However, confirmation of phase purity and accurate phase identification requires comparison of the experimental diffraction pattern with suitable reference or simulated diffraction data**.[17-20]**

3.7.X-ray Photoelectron Spectroscopy of Zn Complex

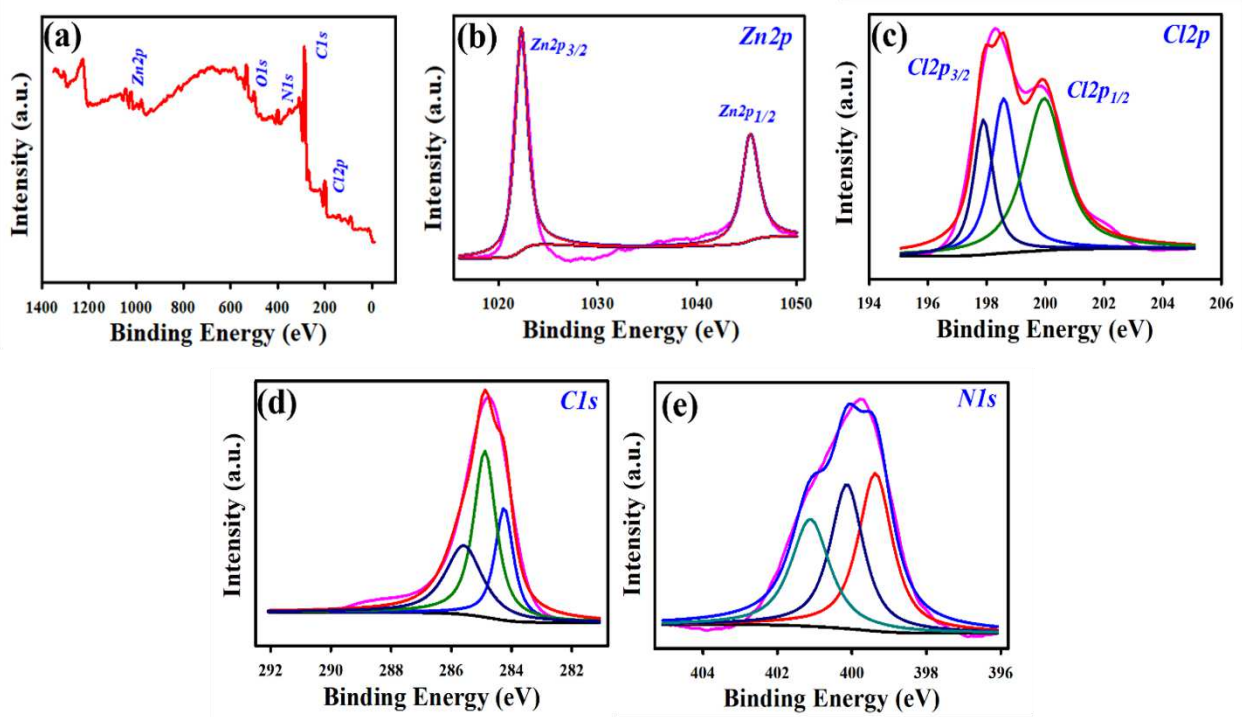


Figure.6. XPS total survey spectrum (a), Zn_{2p} (b), Cl_{2p} (c), C_{1s}(d), and N_{1s}(e)of the synthesized Zn (II) Schiff-base complex.

X-ray photoelectron spectroscopy (XPS) was employed to investigate the surface elemental composition and chemical states of the synthesized Zn (II) Schiff-base complex. The survey spectrum confirmed the presence of carbon (C), nitrogen (N), chlorine (Cl), and zinc (Zn), consistent with the expected composition of the as prepared complex under optimum conditions shown in **Fig.6(a).** In **Fig.6(b)** investigates the Zn 2p spectrum is particularly important for confirming the presence and chemical state of zinc in the complex. The characteristic Zn $2p_{3/2}$ and Zn $2p_{1/2}$ components, typically observed near 1022.48 eV and 1045.58 eV, respectively, are consistent with Zn(II) species, although the precise assignments should be verified against the measured binding energies and complementary evidence. The high-resolution Cl 2p XPS spectrum was recorded to investigate the chemical state and bonding environment of chlorine in the synthesized material. The **Fig.6(c)** shows the Cl 2p spectrum typically exhibits a spin–orbit doublet corresponding to Cl $2p_{3/2}$ and Cl $2p_{1/2}$ components investigates the binding energies of 198.31 eV and 200.06 eV provide insights into the chemical nature of chlorine and its possible interactions with the surrounding chemical species **[21].** The Cl 2p spectrum is associated with chlorine in the 4-chlorophenyl group, provided that the observed signal is consistent with the expected chemical state. The high-resolution C 1s

spectrum can be deconvoluted into components corresponding to aromatic carbon (C–C/C=C) and carbon atoms associated with C=N bonds exhibited in the 283.5-287.68 eV investigates in **Fig.6(d).** The N 1s spectrum provides information about the nitrogen environments originating from the pyridine ring and the imine functionality exhibits in **Fig.6(e).** The binding-energy positions and relative contributions of these components can help to evaluate changes in the nitrogen chemical environment following coordination with Zn (II). **[22-24]**

3.8.Cyclic Voltammetry

Electrochemical Response of $ZnLCl_2$

Cyclic voltammetry (CV) was employed to investigate the electrochemical behavior of the bare GCE and $ZnLCl_2$-modified GCE. The measurements were carried out in 0.1 M phosphate-buffered saline (PBS) at pH 7.0 with a scan rate of 50 mV s^{-1}. As observed in the cyclic voltammograms, the bare GCE exhibited no distinct redox peaks within the investigated potential window, indicating the absence of a noticeable electrochemical response under the selected experimental conditions. In contrast, the $ZnLCl_2$-modified GCE exhibited a distinct anodic peak at −0.296 V, with a maximum oxidation peak current of 15.8 µA. The appearance of this anodic peak demonstrates the electrochemical activity of the $ZnLCl_2$ complex at the modified electrode surface. These results indicate that modification of the GCE with the $ZnLCl_2$ complex introduces an electrochemically active species, resulting in a distinct oxidation response.**[25-27]**

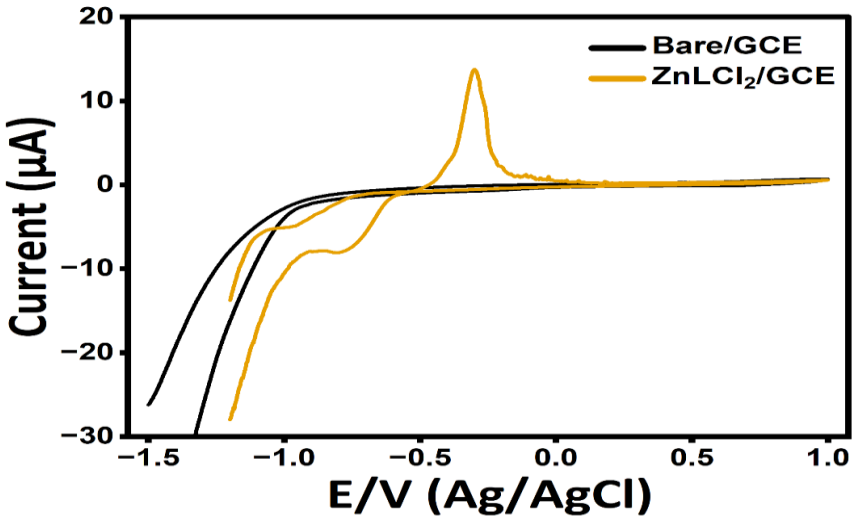


Figure.7. Cyclic voltammograms of the bare GCE and $ZnLCl_2$-modified GCE recorded in 0.1 M PBS (pH 7.0) at a scan rate of 50 mV s^{-1}.

3.9.Analysis of SEM-EDX

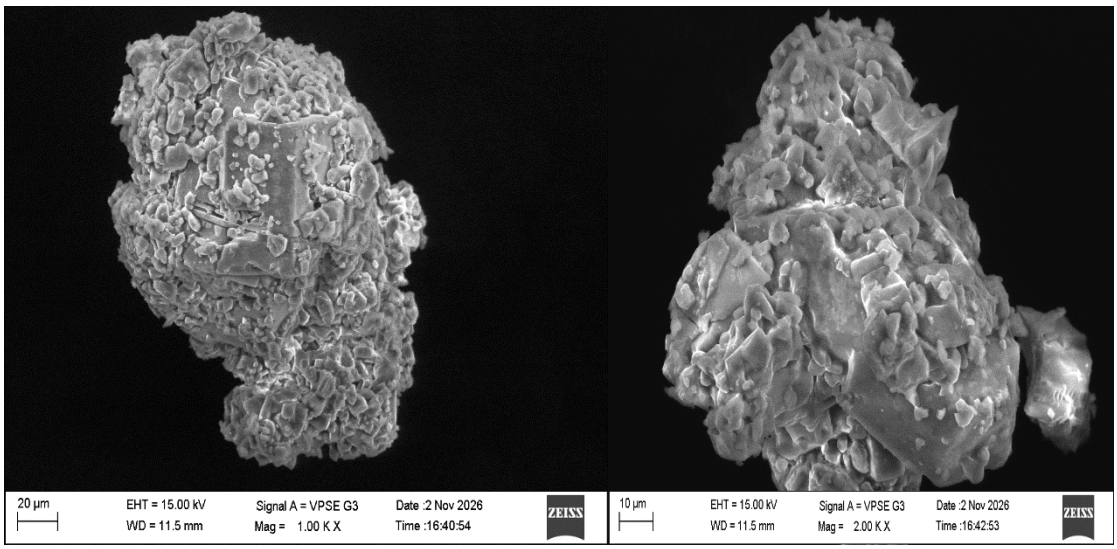


Figure.8. SEM of Zn(II) Metal Complex

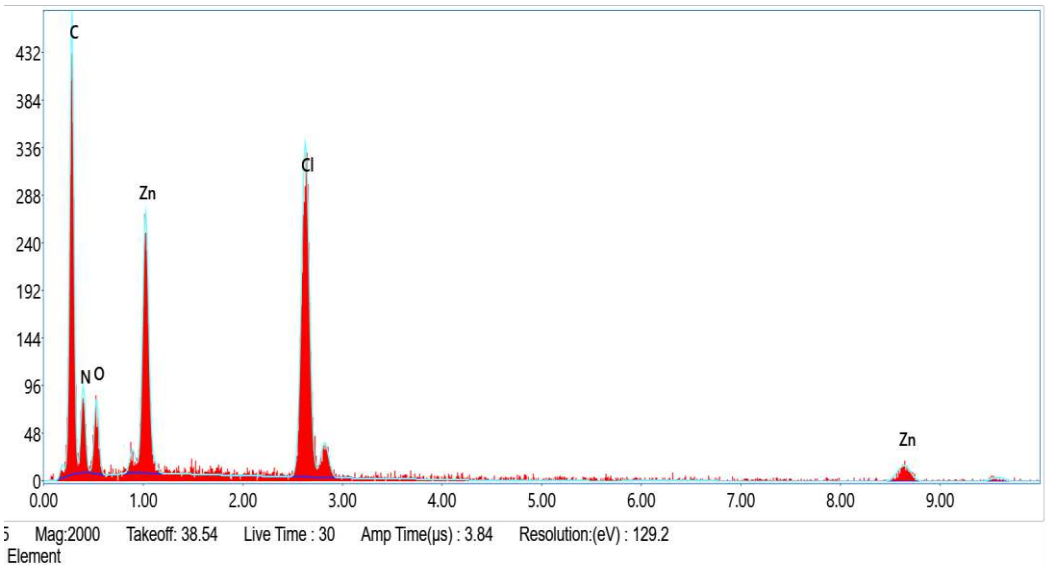


Figure.9. SEM-EDX of Zn(II) Metal Complex

Table.2 SEM–EDX Elemental Analysis of the Zn(II) Schiff-base Metal Complex.

Element	**Weight %**	**Atomic %**
C K	52.0	66.7
N K	16.4	18.1
O K	7.1	6.8
Cl K	13.5	5.8
Zn K	11.0	2.6

The elemental composition of the synthesized Zn (II) Schiff-base complex was investigated using energy-dispersive X-ray (EDX) analysis coupled with scanning electron microscopy

(SEM). The EDX spectrum revealed the presence of carbon (52.0%), nitrogen (16.4%), oxygen (7.1%), chlorine (13.5%) and zinc (11.0%) by weight. The detection of carbon and nitrogen is consistent with the Schiff-base framework, while the presence of chlorine is associated with the 4-chlorophenyl moiety and other chlorine-containing species. The detection of zinc confirms the presence of the metal in the analysed sample. However, the observed oxygen content requires further investigation, as oxygen is not included in the proposed molecular composition of the ligand. Overall, the EDX results provide elemental evidence supporting the presence of zinc and the constituent elements in the analysed sample**. [28-31]**

3.10.TGA Analysis

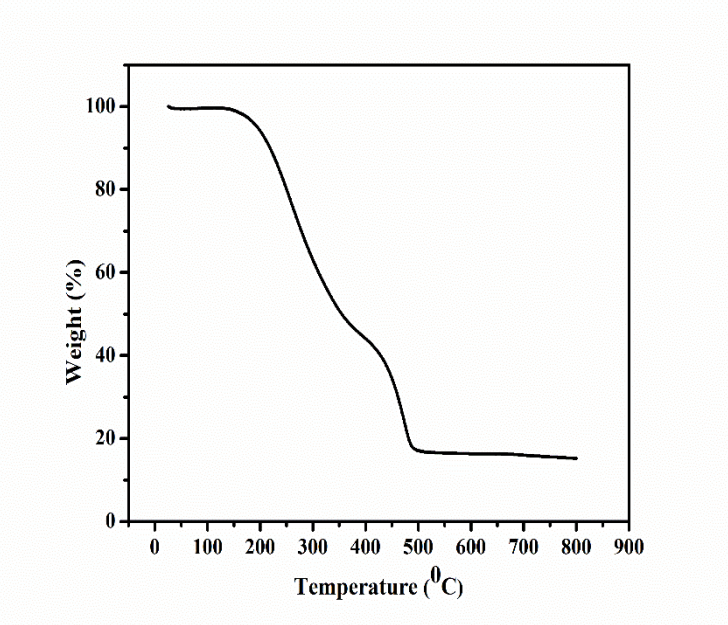


Figure.10 TGA Analysis of Zn(II) Metal Complex

The thermal stability and decomposition behaviour of the synthesized Zn (II) Schiff-base complex were investigated using thermogravimetric analysis (TGA). The thermogram reveals an initial region of thermal stability up to approximately 150 °C, indicating the absence of significant weight loss at lower temperatures. The subsequent decomposition occurs in two major stages. The first stage, observed over approximately 150–420 °C, is associated with the progressive degradation of the organic components of the Schiff-base complex. The second major weight-loss stage occurs between approximately 420 and 500 °C, which can be attributed to further decomposition of the organic ligand framework. Above 500 °C, the thermogram exhibits a nearly constant residual mass of approximately 15–17%, suggesting the formation of a thermally stable inorganic residue. Overall, the TGA results provide information about the

thermal decomposition behaviour and residual stability of the synthesized Zn (II) complex**. [32-34]**

4.Evaluation of Biological Activities

4.1.DPPH radical scavenging assay

The free radical scavenging activity of the ligand and ligand–Zn complex was determined using the stable 2,2-diphenyl-1-picrylhydrazyl (DPPH) radical following the method of Brand, with slight modifications **[35-36].** A 500 µM DPPH solution was prepared in ethanol. For the assay, 100 µL of DPPH solution was mixed with different concentrations of the ligand and ligand–Zn complex, and the reaction volume was adjusted to 1 mL with ethanol. The reaction mixtures were incubated for 24 h in the dark at room temperature. The reduction of the DPPH radical was monitored based on the disappearance of its characteristic purple color, and the absorbance was measured at 517 nm using a spectrophotometer. Ascorbic acid was used as the reference antioxidant.

4.2.Cell viability assay

The cytotoxic effects of the ligand and ligand–Zn complex were assessed in MCF-7 cells using a colorimetric MTT assay. MCF-7 cells obtained from the National Centre for Cell Science (NCCS), Pune, were maintained in DMEM/MEM supplemented with 10% FBS and 1% antibiotic-antimycotic solution at 37 °C under a humidified 5% CO_2 atmosphere. For the cytotoxicity experiment, cells were dispensed into 96-well culture plates at approximately 20,000 cells/well and allowed to establish for 24 h. The cells were subsequently exposed to the ligand and ligand–Zn complex at concentrations of 12.5, 25, 50, 100, and 200 µg/mL and maintained under standard culture conditions for 48 h. Following treatment, the culture medium was removed and MTT reagent was added to obtain a final concentration of 0.5 mg/mL. The plates were protected from light and incubated for 3 h allowing metabolically active cells to convert MTT into insoluble formazan. The resulting crystals were dissolved using 100 µL DMSO, and the absorbance was recorded at 570 nm using a microplate reader **[37].**Cell viability was expressed relative to the untreated control according to the following equation:

$$\text{Cell viability (\%)} = \frac{\text{Mean absorbance of treated cells}}{\text{Mean absorbance of untreated control cells}} \times 100$$

The concentration producing 50% reduction in cell viability (IC_{50}) was determined from the concentration–response relationship by linear regression where applicable.

4.3.Antimicrobial Assay

The antimicrobial activity of the ligand and ligand–Zn complex was evaluated against the bacterial strains *Escherichia coli* and *Pseudomonas aeruginosa* and the fungal strain *Candida albicans* using the agar well-diffusion method **[38].** was prepared in distilled water at pH 7.0 and sterilized by autoclaving at 121 °C for 15 min, followed by pouring into sterile Petri plates and allowing the medium to solidify. Freshly prepared microbial cultures were adjusted to approximately 10^6 CFU/mL and uniformly inoculated onto the MHA surface using a sterile cotton swab. Wells were prepared in the inoculated agar, and the ligand and ligand–Zn complex were added at concentrations of 400, 600, 800, and 1000 µg/mL. Appropriate standard antimicrobial agents, namely chloramphenicol for *E. coli*, tetracycline for *P. aeruginosa*, and fluconazole for *C. albicans*, were used as positive controls. The plates were kept at room temperature for 4 h to facilitate diffusion of the test compounds and subsequently incubated at 37 °C for 24 h. After incubation, the diameter of the resulting zones of inhibition (ZOI) was measured in millimeters.

4.4.Molecular Docking Procedure

Molecular docking studies were performed to investigate the binding affinity and intermolecular interactions of ligand and ligand-Zn complex with estrogen receptor alpha (ERα) and cyclin-dependent kinase 4 (CDK4). The three-dimensional structures of the ligand and Zn complex were prepared using Chemdraw, while the crystal structures of ERα (PDB ID: 3ERT) and CDK4 (PDB ID: 7SJ3) were obtained from the Protein Data Bank **[39].** Protein and ligand structures were prepared using Auto Dock Tools version 1.5.7 prior to docking **[39].**The docking search space was defined using grid boxes of 40 × 40 × 40 points. For ERα, the grid was centered at X = 28.705, Y = 1.533, and Z = 22.406, whereas the CDK4 grid was centered at X = 12.533, Y = −35.924, and Z = 11.31. The selected grid dimensions encompassed the ligand-binding regions of the respective proteins and enabled conformational sampling of the test compounds within the binding pockets. The docking protocol was validated by redocking the ligand present in the respective crystallographic PDB structure into its original binding site. The experimentally determined binding orientation of the co-crystallized ligand was used as the reference conformation, and the predicted pose obtained after redocking was compared with the crystallographic pose. The accuracy of the docking protocol was assessed by calculating the root mean square deviation (RMSD) between the experimental and predicted ligand coordinates. RMSD values below 2 Å were considered indicative of an acceptable reproduction of the experimentally observed binding mode. The validated docking protocol was subsequently applied to ligand and ligand-Zn complex. Docking calculations were

performed using Auto Dock, and the binding conformation with the most favorable predicted docking score was selected for subsequent analysis. Post-docking visualization was performed using PyMOL to examine the orientation of the compounds within the binding pockets and characterize the hydrogen-bonding and hydrophobic interactions responsible for protein–ligand stabilization.

4.5.Antimicrobial activity

The antimicrobial activity of the ligand and ligand–Zn complex was evaluated against the Gram-negative bacterial strains *Escherichia coli* and *Pseudomonas aeruginosa* and the fungal strain *Candida albicans* using the agar well-diffusion method. Both compounds exhibited measurable antimicrobial activity, with the extent of inhibition varying according to the test organism and treatment. Against *E. coli*, the ligand and ligand–Zn complex showed comparable inhibitory effects across the tested concentration range, indicating that Zn complexation did not markedly alter the activity of the ligand against this organism. In contrast, a pronounced enhancement in activity was observed for the ligand–Zn complex against *P. aeruginosa*, where the complex consistently produced substantially larger inhibition zones than the parent ligand and approached the activity of the tetracycline reference at the highest tested concentration. A similar enhancement was observed against *C. albicans*, with the ligand–Zn complex exhibiting considerably greater antifungal activity than the free ligand and producing inhibition comparable to or exceeding that of the fluconazole control at the highest concentration. The concentration-dependent increase in inhibition observed for both compounds, particularly against *P. aeruginosa* and *C. albicans*, indicates a stronger antimicrobial response at increasing concentrations. Overall, the results demonstrate that Zn complexation substantially improved the antimicrobial performance of the ligand, with the most pronounced effects observed against *P. aeruginosa* and *C. albicans*. The corresponding zones of inhibition are presented in **Table 3,** and representative agar well-diffusion plates are shown in **Figure 6.**

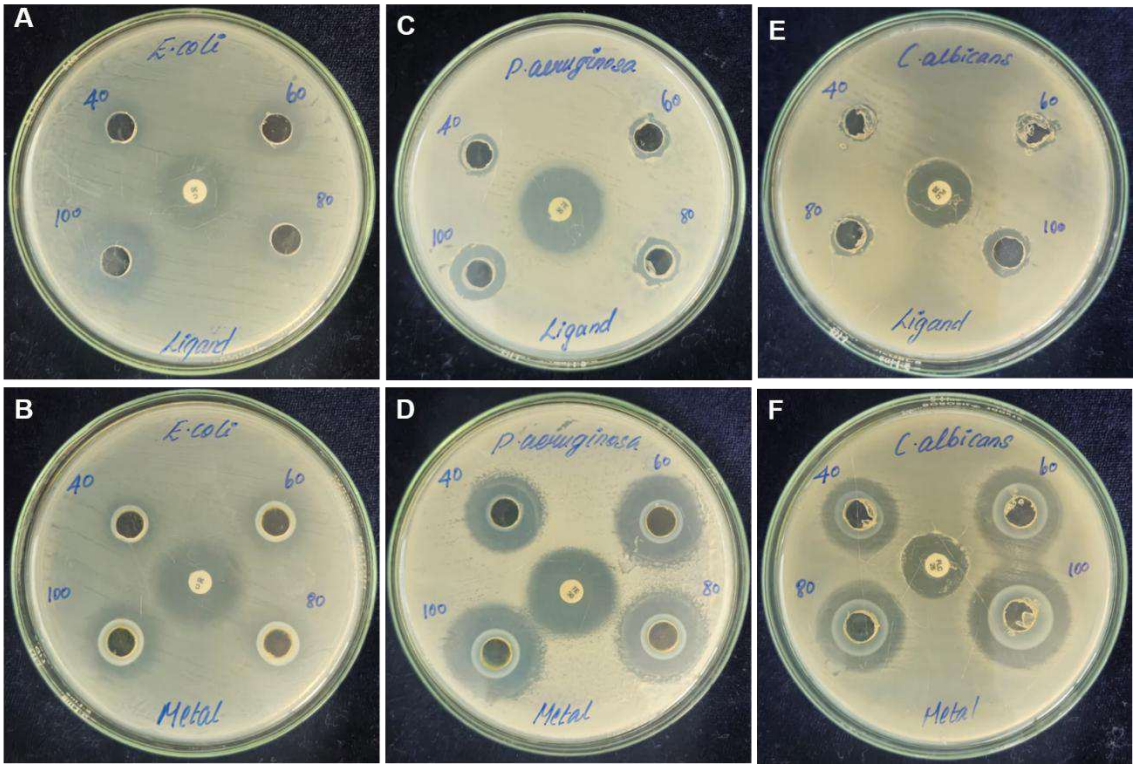


Figure 6. Representative plate image showing ZOI by ligand and ligand-Zn complex against (A and B) *E. coli,* (C and D) *P. aeruginosa,* and (E and F) *C. albicans*

Table 3. Details of ZOI of ligand and ligand-Zn complex against bacteria and fungi

Organism	**Sample**	**Zone of inhibition (mm)**				
		Positive control	**400 µg/mL**	**600 µg/mL**	**800 µg/mL**	**1000 µg/mL**
E. coli	Ligand	Chloramphenicol (29 mm)	11	13	16	22
	Ligand–Zn complex		12	14	16	21
P. aeruginosa	Ligand	Tetracycline (29 mm)	12	13	14	17
	Ligand–Zn complex		22	25	25	29
C. albicans	Ligand	Fluconazole (25 mm)	11	11	12	14
	Ligand–Zn complex		20	22	22	29

4.6.In vitro antioxidant activity

In vitro antioxidant activity of ligand and ligand-Zn complex was measured as DPPH radical scavenging activity. Both the ligand and ligand-Zn complex showed dose-dependent DPPH radical scavenging activity **(Figure 7A and 7B).** The scavenging activity of positive control, ascorbic acid is shown in **Figure 7C.** The ligand-Zn complex showed radical scavenging activity better in comparison to ligand alone. The half-maximal inhibitory concentration (IC50) of ligand-Zn complex was found to be 846.27 µg/mL, whereas for ascorbic acid is 5.68 µg/mL.

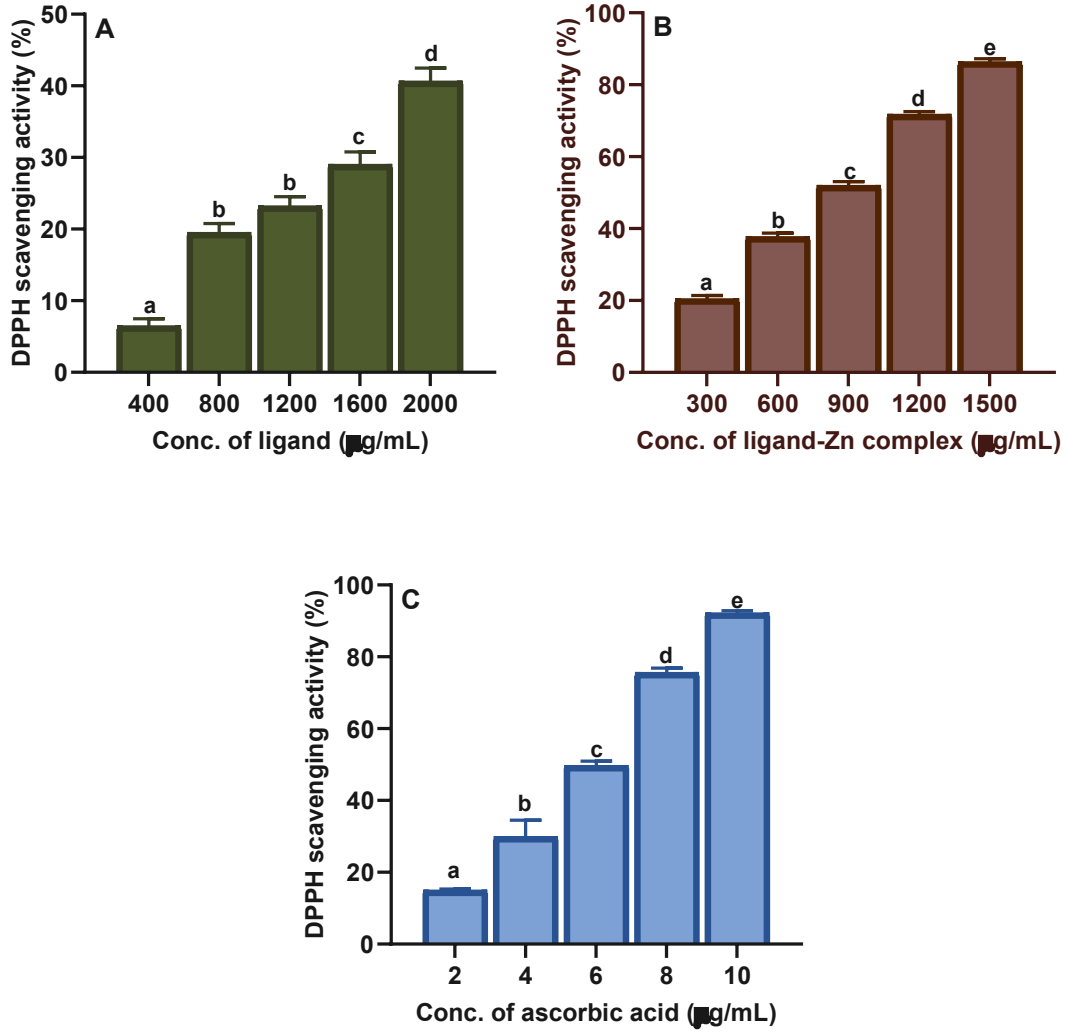


Figure 7. DPPH scavenging activity of (A) ligand, (B) ligand-Zn complex and (C) ascorbic acid. Different letters indicate statistically significant differences (one-way ANOVA with Tukey's post hoc test, $P < 0.05$; n = 3).

4.7.Effect of ligand and ligand–Zn complex on MCF-7 cell viability

The cytotoxic effects of the ligand and ligand–Zn complex on MCF-7 cells were evaluated following 48 h exposure. The ligand produced only a moderate reduction in cell viability over the tested concentration range, with viability remaining above 65% even at the highest concentration tested. Consequently, the ligand did not reach the 50% viability threshold within the investigated concentration range and an IC_{50} value was therefore not applicable.In contrast, treatment with the ligand–Zn complex resulted in a pronounced concentration-dependent reduction in MCF-7 cell viability. Cell viability progressively decreased with increasing concentration, indicating a stronger cytotoxic response toward MCF-7 cells compared with the parent ligand. The calculated IC_{50} value for the ligand–Zn complex was 67.49 µg/mL, demonstrating that Zn complexation considerably increased the cytotoxic potential of the compound against MCF-7 cells.The comparative response of the two compounds indicates that the ligand–Zn complex exhibited substantially greater cytotoxic activity than the free ligand under the experimental conditions. The concentration-dependent are presented in **Figure 8.**

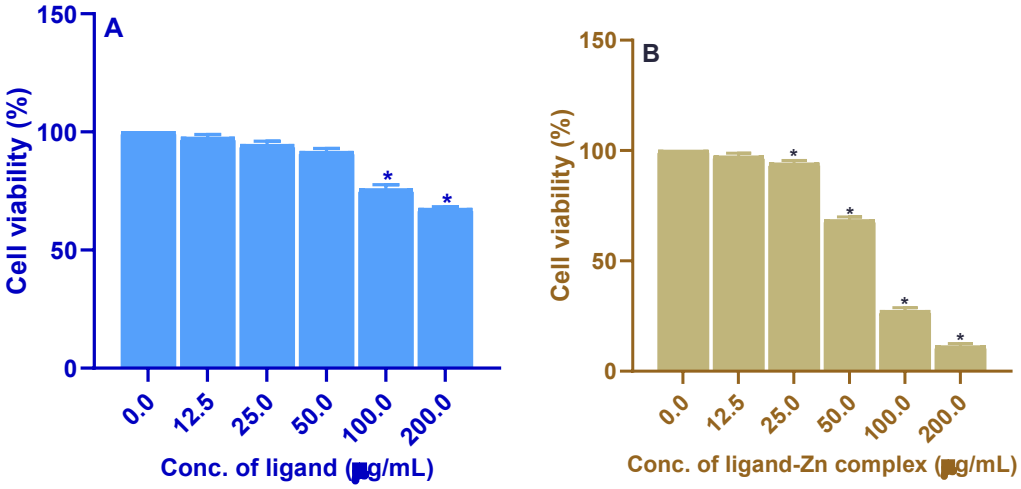


Figure 8. Cytotoxic activity of ligand and ligand-Zn complex in MCF7 cells. Data are presented as mean ± SD (n = 3). Statistical analysis by one-way ANOVA with Tukey's post hoc test, $^{*}P < 0.05$ vs. control.

4.8.Molecular docking analysis

The docking protocol was validated by redocking the respective co-crystallized ligand into the experimentally determined binding site of ERα and CDK4. The resulting RMSD values of 0.217 Å for ERα and 0.229 Å for CDK4 were substantially below the 2 Å acceptance threshold, confirming that the docking protocol was capable of reproducing the experimentally observed ligand-binding orientation with high positional accuracy. The validated protocol was

subsequently used to evaluate the binding modes of ligand and ligand-Zn complex. The molecular docking analysis demonstrated that both ligand and ligand-Zn complex exhibited favorable binding with the selected cancer-related targets ERα and CDK4. Notably, complexation with Zn markedly improved the predicted binding affinity toward both proteins.

4.9.Docking interaction with ERα

The ligand exhibited a favorable interaction with ERα, with a docking score of −6.6 kcal/mol. In comparison, the ligand-Zn complex showed a substantially improved docking score of −9.21 kcal/mol, indicating enhanced predicted binding affinity following Zn complexation. The RMSD obtained for the ERα docking system was 0.217 Å, which was well below the 2 Å criterion used for evaluation of the docking pose. The interaction analysis showed that ligand was stabilized within the ERα binding pocket through hydrogen-bonding interactions involving Leu346, Glu353, Leu387, and Arg394, together with hydrophobic contacts involving Leu346, Leu391, Phe404, and Ile424 **(Table.4).** These interactions indicate that the ligand was accommodated within a predominantly hydrophobic region of the receptor while being further stabilized by polar contacts. Report The ligand-Zn complex exhibited a more extensive interaction network within ERα. Hydrogen-bonding interactions were observed with Leu346, Thr347, Ala350, Leu387, Met388, Gly420, and Gly521, whereas hydrophobic interactions involved Leu346, Ala350, Trp383, Ile424, and Leu525. The increased number and distribution of intermolecular contacts were accompanied by the improved docking score of the Zn complex, suggesting stronger stabilization within the ERα binding pocket. The corresponding interaction poses and binding-pocket orientations are illustrated in **Figure 4A and 4B.**

4.10.Docking interaction with CDK4

Both compounds also showed favorable binding toward CDK4. The ligand exhibited a docking score of −7.04 kcal/mol, whereas the ligand-Zn complex showed a considerably improved docking score of −9.7 kcal/mol. The RMSD value for the CDK4 docking system was 0.229 Å, confirming that the predicted binding orientation was within the acceptable range **[40].**The ligand interacted with CDK4 through hydrogen bonds involving Glu94, Val96, and Gln98, while hydrophobic contacts were observed with Ala33, Val72, Phe93, Val96, and Leu147. These interactions supported the accommodation of the ligand within the CDK4 binding pocket and contributed to its favorable docking score. In comparison, ligand-Zn formed an expanded interaction network with CDK4. Hydrogen-bonding interactions involved Ile12, Tyr17, Glu94, Val96, Asp97, Asp99, and Glu144, while hydrophobic contacts were identified with Ile12, Val20, Lys22, Ala33, Val96, Asp99, and Leu147. The greater extent of intermolecular interactions was associated with the improved docking score of the Zn complex compared with

the parent ligand. The predicted binding orientation and intermolecular contacts are shown in **Figure 4C and 4D.**

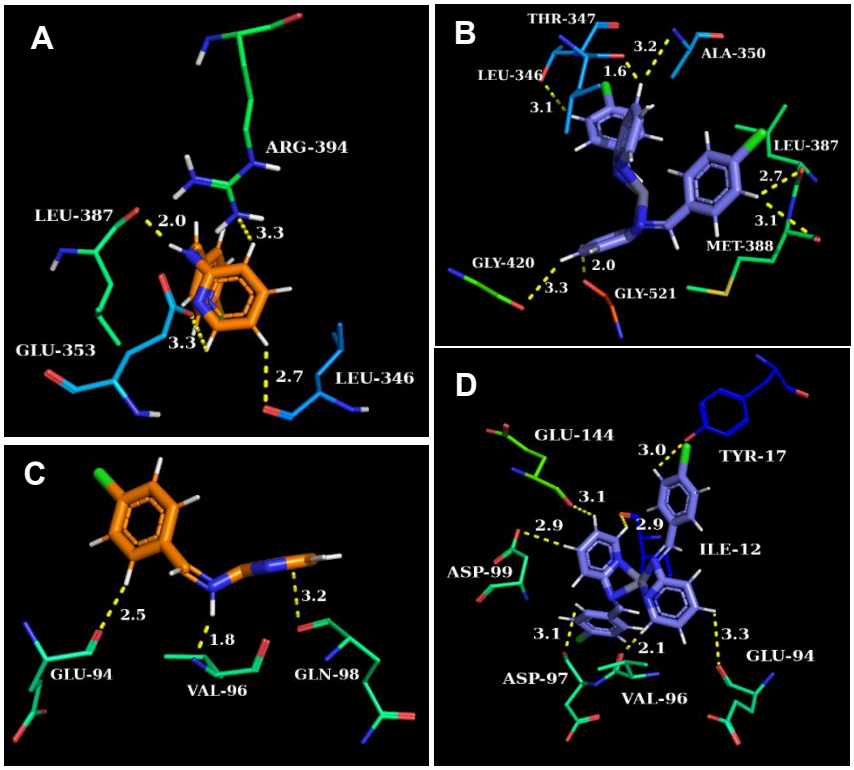


Figure 8. Interaction of ligand and ligand-Zn complex with Erα (A and B) and CDK4 (C and D)

Table 4. Intermolecular interactions of ligand and ligand-Zn complex with BCL2 and $KRAS^{G12D}$ proteins

Ligand – protein complexes	**Hydrogen bonding interactions**	**Hydrophobic interactions**
	Distance (Å)	
Ligand-ERα	Leu346 (2.7), Glu353 (3.3), Leu387 (2.0), Arg394 (3.3)	Leu346 (3.7), Leu391 (3.4), Phe404 (3.6), Ile424 (3.9)
Ligand-Zn complex-ERα	Leu346 (3.1), Thr347 (1.6), Ala350 (3.2), Leu387 (2.7), Met388 (3.1), Gly420 (3.3), Gly521 (2.0)	Leu346 (3.0), Ala350 (3.6), Trp383 (3.2), Ile424 (3.0), Leu525 (3.1)

Ligand- CDK4	Glu94 (2.5), Val96 (1.8), Gln98 (3.2)	Ala33 (3.3), Val72 (3.3), Phe93 (3.5), Val96 (3.8), Leu147 (3.6)
Ligand-Cu complex-CDK4	Ile12 (2.9), Tyr17 (3.0), Glu94 (3.3), Val96 (2.1), Asp97 (3.1), Asp99 (2.9), Glu144 (3.1)	Ile12 (3.3), Val20 (3.4), Lys22 (3.2), Ala33 (3.0), Val96 (3.8), Asp99 (3.2), Leu147 (3.8)

5.Conclusion

In this study, a Schiff base ligand and its corresponding Zn(II) complex were successfully synthesized and characterized using elemental analysis and various spectroscopic techniques, UV-Vis, FTIR, 1H-NMR, 13C-NMR, Mass spectrometry, Powder XRD, TGA,CV and SEM-EDX and X-ray photoelectron spectroscopy to analysis the surface elemental composition and chemical states of the synthesized Zn (II) Schiff-base complex. The spectral and analytical data supported the formation of the Zn(II) complex, and the proposed structure indicated square-planar geometry. Biological investigations revealed that the Zn(II) complex exhibited enhanced activity compared with the free Schiff base ligand. The synthesized complex demonstrated promising antimicrobial and in vitro antioxidant activities, as evaluated by antimicrobial assays and DPPH radical-scavenging analysis. Furthermore, the MTT assay against MCF-7 breast cancer cells revealed notable cytotoxic activity, with the ligand–Zn(II) complex exhibiting an IC_{50} value of 67.49 μg/mL, suggesting that complexation with Zn(II) enhanced the cytotoxic potential of the ligand. Molecular docking studies further supported these findings, with the free ligand and its Zn(II) complex exhibiting docking scores of −7.04 and −9.7 kcal/mol, respectively, indicating a stronger predicted binding affinity for the complex toward the selected biological target. Overall, these findings suggest that Zn(II) complexation may improve the biological properties of the Schiff base ligand. The synthesized complex therefore represents a promising candidate for further investigation in medicinal chemistry, particularly for its antimicrobial, antioxidant, and anticancer potential. However, additional mechanistic studies, toxicity evaluation, and in vivo investigations are required to establish its therapeutic relevance.

Supplementary Information:

No supplementary information is associated with this manuscript.

Acknowledgements:

One of the authors, M. Periyannan, acknowledges that his work was financially supported by the URF (Ref: PU/AD-3/URF Order/011014/2025) from Periyar University, Salem, Tamil Nadu, India.

Author Contributions

"M. Periyannan: Writing – original draft, Methodology, Investigation, Formal analysis. G. Anbarasu: Writing – review & editing, Data curation, Validation. D.Gopi: Formal analysis, Data curation. R. Rajavel: Writing – review & editing, Validation, Supervision, Conceptualization. All authors reviewed the manuscript."

Funding

The authors received no financial support for the research, authorship, and/or publication of this article.

Data Availability

No datasets were generated or analysed during the current study.

Declarations

Competing Interests The authors declare no competing interests.

References :

1. P. Ghanghas, A. Choudhary, D. Kumar, K. Poonia, "Coordination metal complexes with Schiff bases: Useful pharmacophores with comprehensive biological applications," *Inorganic Chemistry Communications* **130**, (2021): 108710.
2. G. Anbarasu, M. Malathy, P. Karthikeyan, R. Rajave., Silica functionalized Cu(II) acetylacetonate Schiff base complex: An efficient catalyst for the oxidative condensation reaction of benzyl alcohol with amines Journal of Solid State Chemistry 253 (2017) 305–312.
3. R. Kumar, et al., "Recent advances in synthesis of heterocyclic Schiff base transition metal complexes and their antimicrobial activities especially antibacterial and antifungal," *Journal of Molecular Structure* **1294**, (2023): 136346.

4. M. S. Aljahdali, A. A. El-Sherif, “Synthesis and Biological Evaluation of Novel Zn(II) and Cd(II) Schiff Base Complexes as Antimicrobial, Antifungal, and Antioxidant Agents,” *Bioinorganic Chemistry and Applications* **2020**, (2020): 8866382.
5. B. Naureen, et al., “Iron(III) and zinc(II) monodentate Schiff base metal complexes: Synthesis, characterisation and biological activities,” *Journal of Molecular Structure* **1231**, (2021): 129946.
6. T. Chowdhury, et al., “Executing a Series of Zinc(II) Complexes of Homologous Schiff Base Ligands for a Comparative Analysis on Hydrolytic, Antioxidant, and Antibacterial Activities,” *ACS Applied Bio Materials* **3**, (2020): 4348–4357.
7. T. Chowdhury, et al., “Unveiling the binding interaction of zinc(II) complexes of homologous Schiff-base ligands on the surface of BSA protein: A combined experimental and theoretical approach,” *Applied Organometallic Chemistry* **34**, (2020): e5556.
8. M. Sen Chowdhury, et al., “Probing the binding interaction of zinc(II) Schiff bases with bovine serum albumin: A spectroscopic and molecular docking study,” *Applied Organometallic Chemistry* **35**, (2021): e6164.
9. K. K. Meena, K. K. Serawat, R. K. Gunsaria, “In Vitro Evaluation of Antifungal Activity of Synthesized Novel Zn(II) Complex with Schiff Base Ligand,” *Indian Journal of Science and Technology* **16**, (2023): 3721–3726.
10. H.Kargar, M. Fallah-Mehrjardi, M.Ashfaq , KS. Munawar, Tahir MN, R. Behjatmanesh-Ardakani, et al. Zn (II) complexes containing O, N, N, O-donor Schiff base ligands: synthesis, crystal structures, spectral investigations, biological activities, theoretical calculations and substitution effect on structures. J Coord Chem. 2021;74(16):2720–2740.
11. E. S. Aazam, M. Majrashi, M. A. Hussien, “Exploring novel NH-form resorcinol-based Schiff base and its metal complexes: Synthesis, characterization, cytotoxic activity, molecular docking and ADME studies,” *Heliyon* **10**, (2024): e37385.
12. R. K. Al-Shemary, et al., “Synthesis, structural investigations, XRD, DFT, anticancer and molecular docking study of a series of thiazole based Schiff base metal complexes,” *Journal of Molecular Structure* **1275**, (2023): 134676.
13. J. Zhang, L. Xu, W.-Y. Wong, Energy materials based on metal Schiff base complexes, Coord. Chem. Rev., 355 (2018), pp. 180-198, 10.1016/j.ccr.2017.08.007.
14. H. Köksal, M. Dolaz, M. Tümer, S. Serin, Copper (II), cobalt (III), nickel (II), palladium (II), and zinc (II) complexes of the Schiff base ligands derived from 2, 6-

diacetylpyridine and phthaldialdehyde, Synth. React. Inorg. Met., 31 (2001), pp. 1141-1162.

15. A.Ben Rached, W. Maalej, P. Guionneau, N. Daro, T. Mhiri, H.Feki , Z.Elaoud . Synthesis, crystal structure, and vibrational and DFT simulation studies of benzyl ammonium dihydrogen phosphite. J Phys Chem Solids. 2018; 123:150–156.
16. S.M. Obaid, F.H. Ghanim, A.A.S. Al-Hamdani, Synthesis, spectroscopic, characterization and biological activities of Schiff base ligand and metal complexes of some metal (II) salts with anthranilic acid, Res. J. of Pharm. Biol. Chem. Sci., 10 (1) (2019), pp. 1121-1131.
17. Z.-Q. Feng, X.-L. Yang, Y.-F. Ye, Pd(II) and Zn(II) based complexes with Schiff base ligands: Synthesis, characterization, luminescence, and antibacterial and catalytic activities, The Scientific World Journal (2013) Article 956840.
18. M. Abou Melha et al., Spectral, molecular modelling, and biological activity studies on new Schiff's base of acenaphthoquinone transition metal complexes, Bioinorganic Chemistry and Applications (2021).
19. J. D. Chellaian et al., Co(II), Ni(II), Cu(II), and Zn(II) complexes of 4-aminoantipyrine-derived Schiff base: Synthesis, structural elucidation, thermal, biological studies, and photocatalytic activity, Journal of Heterocyclic Chemistry (2021).
20. V. Pushpanathan, S.S.J. Dhas, D.S. Kumar, Investigation on the substituent effects of homodinuclear cobalt(II) complexes of tetraiminediphenol macrocycle on the synthesis of pure Co_3O_4 nanoparticles, Bull. Mater. Sci. 44 (2021) 1–12.)
21. Ain QU, U. Rasheed,Z. Chen, Tong Z. J Hazard Mater. 2024; 476:135009
22. N.Z. Nor Hashim, K. Kassim, H.M. Mohd Zaki, XPS Characterization on Benzylidene Schiff Base Ligand, ARPN Journal of Engineering and Applied Sciences 11(16) (2016).
23. L.-W. Xue, X. Fu, G.-Q. Zhao, Q.-B. Li, Zinc(II) complexes derived from Schiff bases: Syntheses, structures, and biological activity, Acta Chimica Slovenica 68(1) (2021) 17–24.
24. M. Azam et al., Zn(II) complex derived from bidentate Schiff base ligand: Synthesis, characterization, DFT studies and evaluation of anti-inflammatory activity, Journal of Molecular Structure 1201 (2020), Article 127177.)
25. H.Kargar , et al. Synthesis, characterization, electrochemical, and theoretical investigation of nitro-substituted salophen Schiff base complexes. Inorg Chim Acta. 2026; 590:122984

26. Mini P.S.S.P., Antony R., Manickam S.T.D., Thanikaikarasan S., Subramanian R., Balakumar S., Mahalingam T., Saldana S., Ixtlilco L.: Synthesis, characterization and electrochemical properties of Schiff base complexes derived from amino acids. J. New Mater. Electrochem. Syst. 17(3), 179–183 (2014).
27. M.Montazerozohori,S.Yadegari,A. Naghiha,S.Veyseh. Synthesis, Characterization, Electrochemical Behavior, Thermal Study and Antibacterial/Antifungal Properties of Some New Zinc(II) Coordination Compounds. J. Ind. Eng. Chem. 2014, 20 (1), 118–126.
28. D.Mariyam; N.Farida,;H.W. Wijaya; I.Dasna,W. Studi Karakterisasi dan Aktivitas Antibakteri Senyawa Kompleks dari Zink(II) Klorida, Kalium Tiosianat dan 2-Aminopiridina. J. Ris. Kim. 2022, 13 (1), 100–110.
29. P.Kavitha,;K.L. Reddy,Synthesis, Spectral Characterisation, Morphology, Biological Activity and DNA Cleavage Studies of Metal Complexes with Chromone Schiff Base. Arabian Journal of Chemistry 2016, 9 (4), 596–605.
30. M.Hanif; N.Kosar; T.Mahmood; M.Muhammad,;F. Ullah; M.N.Tahir; A.I.Ribeiro, E.Khan.Schiff Bases Derived from 2-Amino-6-methylbenzothiazole, 2-Amino-5-chloropyridine and 4-Chlorobenzaldehyde: Structure, Computational Studies and Evaluation of Biological Activity. ChemistrySelect 2022, 7 (38), e202203386.
31. R.S.Joseyphus;M.S. Nair. Antibacterial and Antifungal Studies on Some Schiff Base Complexes of Zinc(II). Mycobiology 2008, 36 (2), 93–98.
32. D.Osypiuk,A.Bartyzel, B.Cristóvão: Synthesis, thermal behaviour and evaluation of the antioxidant capacity of Zn (II) complexes with polydentate Schiff bases. J. Mol. Struct. 1294, 136337 (2023).
33. MD.Nisargandh , SM.Annapure , JV.Bharad. Synthesis, characterization, thermal, X-ray and antimicrobial study of Zn (II) metal complexes of dehydroacetic acid-based new Schiff bases. J Adv Sci Res. 2022;13(3):107-111.
34. N.Kavitha, PV.Anantha Lakshmi. Synthesis, characterization and thermogravimetric analysis of Co (II), Ni (II), Cu (II) and Zn (II) complexes supported by ONNO tetradentate Schiff base ligand derived from hydrazino benzoxazine. J Saudi Chem Soc. 2017;21(Suppl 1).
35. K.Arunachalam,PS.Sreeja. MTT assay protocol. Advanced cell and molecular techniques: protocols for in vitro and in vivo studies: Springer; 2025. p. 271-6.

36. W.Brand-Williams, M.E.Cuvelier, C.Berset: Use of a free radical method to evaluate antioxidant activity. LWT – Food Sci. Technol. 28, 25–30 (1995).
37. SI.Gharbi, LA.Pelletier, A.Espada, J.Gutiérrez, SMG.Sanfeliciano,CT. Rauch, et al. Crystal structure of active CDK4-cyclin D and mechanistic basis for abemaciclib efficacy. NPJ Breast Cancer. 2022;8:126
38. GM.Morris,R.Huey,W.Lindstrom,MF.Sanner,RK.Belew,DS.Goodsell, et al. AutoDock4 and AutoDockTools4: Automated docking with selective receptor flexibility. Journal of computational chemistry. 2009;30:2785-91.
39. AK.Shiau ,D. Barstad ,PM. Loria , L.Cheng , PJ.Kushner , DA.Agard, et al. The structural basis of estrogen receptor/coactivator recognition and the antagonism of this interaction by tamoxifen. Cell. 1998;95:927-37.
40. K.M.Tawfiq , A.J. Al-Sarray, H.A.S. Al-Naymi, S.M.H. Obaid.,A.J. Jarad, R.A.Hashim: Synthesis, characterization, molecular docking, cytotoxicity, and antimicrobial activity of Schiff base ligand and its metal complexes. J. Mol. Struct. 1355, 144997 (2026).